Diminished adherence of snail hemocytes to schistosome sporocysts of *Schistosoma mansoni* following programmed knockout of the allograft inflammatory factor of *Biomphalaria glabrata*

Fernanda Sales Coelho[1], Rutchanee Rodpai[2,3] André Miller[4], Shannon E Karinshak[2,5], Victoria H Mann[2,5], Omar dos Santos Carvalho[1], Roberta Lima Caldeira[1], Marina de Moraes Mourão[1*], Paul J Brindley[2,5*], Wannaporn Ittiprasert[2,5*]

[1] Grupo de Pesquisa em Helmintologia e Malacologia Médica, Centro de Pesquisas René Rachou, Fundação Oswaldo Cruz, Belo Horizonte, MG, Brasil.
[2] Department of Microbiology, Immunology and Tropical Medicine, School of Medicine and Health Sciences, George Washington University, Washington, D.C., USA
[3] Department of Parasitology, Faculty of Medicine, Khon Kaen University, Khon Kaen, 40002 Thailand.
[4] Biomedical Research Institute , Schistosomiasis Resource Center, Rockville, MD, USA
[5] Research Center for Neglected Diseases of Poverty, School of Medicine and Health Sciences, George Washington University, Washington, D.C., USA

Schistosomiasis mansoni is a debilitating neglected tropical disease caused by infection with the blood fluke, *Schistosoma mansoni*. Development of the larval stage of the parasite in an intermediate host snail of the genus *Biomphalaria* is an obligatory component of the life cycle. Enhanced understanding of the mechanism(s) of host defense in the intermediate host snail may hasten the development of new tools that block transmission of schistosomiasis. The embryonic cell line from *B. glabrata*, termed the Bge line, is a versatile resource in the investigation of snail-schistosome interactions. A key attribute of the Bge cell is its hemocyte-like phenotype, given the central role of the snail hemocyte in innate and cellular immunity. The allograft inflammatory factor 1 (AIF, *aif*) is a conserved antigen typically expressed in phagocytic and granular leukocytes and is a marker of macrophage activation. AIF is highly expressed in isolates of *B. glabrata* that are resistant to infection with *S. mansoni*. We targeted the *aif* gene of *B. glabrata* (*Bg*AIF) for programmed gene knockout using the CRISPR/Cas9 approach, to investigate the activity of CRISPR/Cas9 gene editing in this gastropod species and, in turn, to investigate the loss of AIF on Bge cell-mediated adherence to schistosome sporocysts. Bge cells were transformed with gene editing plasmid encoding the Cas9 nuclease driven by the CMV promoter and a guide RNA specific for exon 4 of the *Bg*AIF by square wave electroporation. Twelve independent transformations were carried out. Transcript levels of *Bg*AIF were significantly reduced by up to 73% (range, 26 to 73%; mean 49.5±20.2% S.D; n = 12) from two to nine days following transformation. Sanger direct sequencing and bioinformatic analysis of the sequence reads revealed on-target programmed mutation on the *Bg*AIF gene, including insertions of 1-2 bp and deletion of 8-30 bp, (range, 9 to 17% of *Bg*AIF gene; n =12). In addition, the adherence of gene-edited Bge cells to sporocysts was significantly impeded in comparison to control cells, as ascertained using the cell adherence index (CAI); 2.66±0.10 (control) *vs.* 2.30±0.22 (Δ*Bg*AIF cells), $P < 0.05$. This is the first report of gene editing in this medically important taxon of freshwater gastropods that are necessary for the transmission of schistosomiasis.

Keywords: Biomphalaria glabrata embryonic cell line; CRISPR/Cas9; gene editing; allograft inflammatory factor, cell adhesion

**correspondence; equal contribution*

Wannaporn Ittiprasert, email, wannaporni@gwu.edu; Paul J. Brindley, email, pbrindley@gwu.edu; Marina de Moraes Mourão, email, marina.mourao@fiocruz.br

Introduction

Schistosomes evolved a complex developmental cycle, which includes both a freshwater gastropod intermediate host and a definitive mammalian host. Several species of the freshwater snail genus *Biomphalaria* are intermediate host for *Schistosoma mansoni* in South America and the Caribbean. The neotropical species *Biomphalaria glabrata* has been investigated extensively with respect to host-parasite relationship and coevolution with *S. mansoni* especially on mechanisms of susceptibility and/or resistance to the compatible parasites (Webster & Davies, 2001; El-Ansary & Al-Daihan, 2006). Genetic variation is evident among isolates and strains of *B. glabrata*, both in the laboratory and field settings, resulting in a spectrum of susceptibility of infection with *S. mansoni* (Richards & Shade, 1987). Considerable advances have been made in order to explore the determinant mechanisms of parasite susceptible and resistant snails for their internal defense system (Knight *et al.*, 2011; Jannotti-Passos *et al.*, 2008; Hanington *et al.*, 2010; Pila *et al.*, 2016; Zhang *et al.*, 2008; Lockyer *et al.*, 2012; Larson *et al.*, 2014; Pinaud *et al.*, 2016; Barbosa *et al.*, 2006). The resistance phenotype is underpinned by a dominant genetic trait, where the schistosome larva fails to develop as the consequence of innate and cellular immune responses. Hemolymph and hemocytes in resistant snails encapsulate and destroy the sporocyst (Barbosa *et al.*, 2006; Adema & Loker, 2015; Coustau *et al.*, 2015; Mitta *et al.*, 2017; Pila *et al.*, 2017; Knight *et al.*, 2014; Famakinde, 2017).

The invertebrate cell line, Bge, from the freshwater gastropod *B. glabrata* (Yescott & Hansen, 1976) remains to date the only established cell line from any mollusk. The cell line originates from five-day-old embryos of an isolate of *B. glabrata* susceptible to infection with *S. mansoni*. The Bge cell line has been studied extensively to interrogate the host-parasite relationship because Bge exhibits a hemocyte-like behavior that includes encapsulation of the larval parasite (Laursen & Yoshino, 1999; Wheeler *et al.*, 2018a; Wheeler *et al.*, 2018b; Rinaldi *et al.*, 2015; Odoemelam *et al.*, 2009; Vermeire *et al.*, 2004; Castillo & Yoshino, 2002; Humphries *et al.*, 2001; Yoshino & Laursen, 1995). A draft genome of *B. glabrata* has been reported (Adema *et al.*, 2017), and ongoing transcriptome and proteome catalogues including factors participating in immunological surveillance, phagocytosis and cytokine responses, and also pathogen recognition receptor elements including Toll-like receptors and fibrinogen-related proteins (Adema *et al.*, 2017). An orthologue of the evolutionary conserved allograft inhibition factor, AIF, also plays a key role in the protective response by *B. glabrata* to invasion by larval schistosomes (Lockyer *et al.*, 2012; Larson *et al.*, 2014). The AIF of *B. glabrata*, *Bg*AIF, in like fashion to orthologues in mammals and other taxa, is expressed in hemocytes, which are phagocytic and participate in cellular proliferation and migration. Elevated expression of *Bg*AIF is a characteristic of the resistance of *B. glabrata* to schistosome infection and is a marker of hemocyte activation (Lockyer *et al.*, 2012; Larson *et al.*, 2014). Expression of AIF also is seen during hemocyte activation in oysters (Zhang *et al.*, 2013) and during hepatic inflammation during murine schistosomiasis (Chen *et al.*, 2014; Chen *et al.*, 2012).

The goal of this study was to establish whether programmed genome editing by the CRISPR/Cas9 approach (Doudna & Charpentier, 2014; Jiang & Doudna, 2017; Cong *et al.*, 2013) was functional in *B. glabrata* and, if so, to showcase its use in functional genomics investigation of the host-parasite relationship. Given the role of hemocytes of *B. glabrata* in encapsulation of the sporocyst during cellular responses to schistosome infection, we undertook genetic manipulation of Bge cells as a surrogate for the snail at large. Specifically, we targeted

the *Bg*AIF locus, both as a model gene for the genome of *B. glabrata* generally and because of the role of elevated expression of AIF as characteristic of the resistance to schistosome infection phenotype of *B. glabrata*. As presented below, programmed genome editing was active in the Bge cell and hence, we predict in *B. glabrata*. Moreover, functional genetic knock-out of *Bg*AIF impeded adherence of Bge cells to the primary sporocyst of *S. mansoni*.

Materials and Methods

Gene editing construct

The gene encoding the allograft inflammatory factor of *B. glabrata*, *Bg*AIF (2,226 bp; accession number BGLB005061, https://www.vectorbase.org/) includes five exons interrupted by four introns (Fig. 1A). A guide RNA (gRNA) for Cas9-catalyzed gene editing specific for the target *B. glabrata* gene locus, *Bg*AIF, was identified in the BGLB005061 sequence using the 'CHOPCHOP' v3 tool, https://chopchop.cbu.uib.no/, with default parameters compatible for the protospacer adjacent motif, NGG, of Cas9 from *Streptococcus pyogenes* (Labun *et al.*, 2019; Labun *et al.*, 2016; Montague *et al.*, 2014). Based on the guidance from the CHOPCHOP analysis, we located a gRNA, AGACTTTGTTAGGATGATGC, specific for exon 4 of the *aif* gene, with predicted high CRISPR/Cas9 efficiency for double stranded DNA cleavage in tandem with an absence of off-target activity anywhere else in the genome of *B. glabrata* (Fig. 1A). A CRISPR/Cas9 vector encoding gRNA targeting exon 4 of *Bg*AIF under the control of the mammalian U6 promoter and encoding Cas 9 (with nuclear localization signals1 and 2) driven by the CMV promoter was assembled using the GeneArt CRISPR Nuclease Vector system (Thermo Fisher Scientific, Waltham, MA), according to the manufacturer's protocol, and termed pCas-*Bg*AIFx4 (Fig. 1B). Competent *E. coli* DH5α cells (Invitrogen, Thermo Fisher Scientific) were transformed with pCas-*Bg*AIFx4 by the heat shock method and cultured on LB-agar supplemented with ampicillin at 50 µg/ml. Subsequently, plasmids recovered from several single colonies of ampicillin-resistant *E. coli* transformants were investigated by amplicon PCR-based Sanger direct nucleotide sequence analysis using a U6 gene-specific primer to confirm the integrity of inserted gRNA sequence (Fig. 1B).

Biomphalaria glabrata embryonic (Bge) cell line culture

The Bge cell line was provided by the Schistosomiasis Resource Center (SRC), Biomedical Research Institute (BRI), Rockville, MD. Historically, the Bge cell line was provided to the SRC by the American Type Culture Collection (Manassas, VA), catalogue no. ATCC CRL 1494, and thereafter maintained at BRI for >10 years. Bge cells were maintained at 26ºC in air in 'Bge medium', which is comprised of 22% (v/v) Schneider's *Drosophila* medium, 0.13% galactose, 0.45% lactalbumin hydrolysate, 0.5% (v/v) phenol red solution, 20 µg/ml gentamycin, and supplemented with 10% heat-inactivated fetal bovine serum (Rinaldi *et al.*, 2015; Odoemelam *et al.*, 2009). Bge cells were grown to 80% confluence before transfection by electroporation with pCas-*Bg*AIFx4. The Bge cells were free of contamination with *Mycoplasma*, as established with a PCR-based test (LookOut® Mycoplasma PCR Detection kit, Sigma-Aldrich, St. Louis, MO).

Transfection of Bge cells by square wave electroporation

Bge cells were harvested using a cell scraper, washed twice in Bge medium, counted, and resuspended at 20,000 cell/µl in Opti-MEM medium (Sigma-Aldrich, St. Louis, MO). Two

million cells were transferred into 0.2 mm path length electroporation cuvettes (BTX Harvard Apparatus, Hollister, MA) containing 6 µg pCas-*Bg*AIFx4 in ~100 µl Opti-MEM. The cells were subjected to electroporation using one pulse at 125 volts for 20 milliseconds, using a square wave pulse generator (ECM 830, BTX Harvard Apparatus). Immediately thereafter, the Bge cells maintained in 12-well plates (Greiner Bio-One) at 26ºC. The mock control included Opti-MEM only for electroporation. The presence of transcripts encoding the *B. glabrata* actin (*Bg*Actin) and the Cas9 was monitored daily for nine days following transfection by electroporation (Fig. 1C).

Sequential isolation of total RNA and genomic DNA

To monitor the transfection of Bge cell by pCas9-*Bg*AIFx4 and expression of the expression of Cas9, both total RNA and genomic DNA were extracted sequentially from cell pellets, as previously described (Arunsan *et al.*, 2019; Ittiprasert *et al.*, 2019). In brief, each sample of total RNA sample was extracted using the RNAzol® RT reagent (Molecular Research Center, Inc., Cincinnati, OH) according to the manufacturer's protocol. Subsequently, the DNA/protein pellet retained after recovery of RNA was resuspend in DNAzol® solution (Molecular Research Center, Inc), and total DNA recovered. The samples of RNA and DNA were dissolved in nuclease-free water and concentration and purity established by spectrophotometry (Nanodrop 1000, Thermo Fisher Scientific).

Expression of Cas9 by Bge cells

To investigate transcription from the pCas-*Bg*AIFx4 vector following transfection of Bge cells, levels of transcribed Cas9 were investigated by semi-quantitative RT-PCR. Total RNA from the wild type (WT), mock (Opti-MEM electroporated-) and pCas-*Bg*AIFx4 DNA electroporated-Bge cells was treated with DNaseI enzyme (Ambion, Thermo Fisher Scientific) to remove residual vector pCas-*Bg*AIFx4 and contaminating genomic DNA. The RNAs were reverse transcribed to cDNA using the First Strand cDNA Synthesis kit (New England Biolabs, Ipswich, MA). Quantitative PCRs specific for the actin gene of *B. glabrata*, *Bg*Actin and for the Cas9 coding sequence were carried out, with primer pairs as follows: *Bg*Actin, actin-F: 5'-GTCTCCCACACTGTACCTATC-3' and actin-R: 5'- CGGTCTGCATCTCGTTTT-3'; Cas9, Cas9-F: 5'- GAGTGAACTTCCCGCCGAAT-3' and Cas9-R: 5'-GGTCTTGACGAGACGATGCT-3' (Fig. 1B). Amplicons and molecular size standards were separated by electrophoresis through Tris-acetate-EDTA-buffered agarose (1%) and stained with ethidium bromide (Fig. 1C).

Analysis of programmed mutation of the allograft inflammatory factor gene of *B. glabrata*

Genomic DNA samples from the WT, mock-transfected and pCas-*Bg*AIFx4-transfected cells were amplified by PCR using AIF-F and AIF-R primers that flank the CRISPR/Cas9 programmed double strand break (DSB) site (Fig. 1A). Amplicons were isolated using the PCR cleanup and gel extraction kit (ClonTech, Takara USA, Mountain View, CA) and the nucleotide sequence of amplicons determined by Sanger direct sequencing (GENEWIZ, South Plainfield, NJ). Chromatograms of the sequence reads from all three groups in each experiment were subjected to online analysis using the TIDE algorithm, https://tide.deskgen.com/ (Brinkman & van Steensel, 2019; Brinkman *et al.*, 2018) and also by Inference of CRISPR v2 Edits analysis (ICE) software, https://ice.synthego.com/#/ (Synthego Corporation, Redwood City, CA) (Hsiau

et al., 2018). Estimates of CRISPR efficiency, insertion-deletion (INDEL)-substitution percentages, and the nucleotide sequence of mutant alleles were obtained using both the TIDE and the ICE platforms (Fig. 2A, 2B).

Quantitative real time PCR analysis of transcription of *Bg*AIF

To evaluate the differential levels of the *Bg*AIF transcript among the groups, total RNA was extracted and treated with DNaseI, as above. DNaseI treated-RNA (200 ng) was reverse transcribed to cDNA, followed by quantitative RT-PCR, using the Vii7 real time PCR system (Applied Biosystems, Scientific), and the SSoAdvanced Universal SYBR Green Supermix reagents (Bio-Rad), according to the manufacturer's recommendations. The following nucleotide primers were used: *Bg*AIF specific forward primer, 5'-CCTGCTTTTAACCCGACAGA-3' and reverse primer, 5'-TGAATGAAAGCTCCTCGTCA-3'. Differential expression of *Bg*AIF expression in were calculated after normalizing with *Bg*Actin (primers as above) and comparison with the two control groups. The ΔΔCt method was used to calculate the differential gene expression (Livak & Schmittgen, 2001), with assistance of the GraphPad Prism software (San Diego, CA) (Fig. 2C).

Schistosome sporocysts

Miracidia of NMRI stain *S. mansoni* were hatched from eggs from infected mice (SRC, Biomedical Research Institute, Rockville, MD) under axenic conditions (Yoshino & Laursen, 1995), after which transformation from miracidium to primary sporocyst *in vitro* proceeded, as described (Castillo & Yoshino, 2002). Briefly, hatched miracidia were chilled on ice for 25 min, pelleted by centrifugation, 500*g* at 4°C, 60 sec, to immobilize the larvae. The miracidia were washed with ice cold Chernin's balanced salt solution with 1mg/ml of glucose and trehalose and antibiotic, 10 µl/ml of 100× penicillin/streptomycin (Thermo Fisher Scientific), termed CBSS+. Approximately 5,000 miracidia per well of 24-well plate were cultured in CBSS+ at 26°C for 24 hrs, after which the sporocysts were washed remove shed ciliated epidermal plates and other debris, followed by transfer to a 1.5 ml microcentrifuge tube (Castillo & Yoshino, 2002).

Sporocyst-Bge cell binding assay and cell adhesion index (CAI)

To investigate the ability of cell activation/adhesion by wild type Bge cell *vs. Bg*AIF depleted-cell (Δ*Bg*AIF-Bge), we used the sporocyst-Bge cell binding assay and associated cell adhesion index (CAI), originally reported by Bayne *et al*., 1984 (Bayne *et al.*, 1984). CAI is semi-quantitative measure of performance, with scaling from one to four for increasing adhesion of Bge cells to co-cultured sporocysts (Castillo & Yoshino, 2002; Bayne *et al.*, 1984). In brief, Bge cells were resuspended in CBSS+ medium. In parallel, primary sporocysts were transferred to 1.5 ml siliconized micro-test tubes (Bio Plas, Thomas Scientific, Swedesboro, NJ) and washed three times with CBSS+ by centrifugation at 500 *g* at 4°C, 60 sec each wash. Subsequently, Bge cells were transferred to the siliconized tubes with the sporocysts, at a Bge cell to sporocyst density of 500,000 cells per 200 sporocysts in 200 µl medium. The co-culture was maintained at 26°C in air for 24 hrs, after which the co-cultured sporocysts and Bge cells were transferred, as gently as feasible, to wells of 24-well tissue culture plates (Greiner Bio-One) to score the cell adhesion index. Here, ≥50 sporocysts were counted (using three technical replicates for each count). Seven discrete replicates were performed, *i.e.*, Bge cells were transformed with > 400

sporocysts of each group treatment in each of these biological replicates. The binding scores were independently graded from each well of the plates, by examination using an inverted microscope at 20× magnification (Zeiss Axio Observer A1, Carl Zeiss LLC, White Plains, NY). The CAI values were calculated by total binding value (range from one to four; examples presented in Fig. 3A) divided per the number of sporocysts, according to the formula, CAI = total binding value per number of sporocyst (Castillo & Yoshino, 2002).

Biological replicates

The assay was repeated 12 times, *i.e.*, groups of Bge cells were transfected with the gene-editing plasmid, mock treated, or not treated (WT) on 12 occasions. Gene editing efficacy was examined on each of these 12 biological replicates (termed experiments number 1 to 12) using quantitative RT-PCR and ICE and TIDER analysis, as detailed above. In addition, analysis of the cell adherence index was carried out on seven discrete occasions, using the cells from experiments number 6 to 12 (above). Statistical analysis was undertaken using Prism (GraphPad Software).

Results

Transcription of Cas9 nuclease in Bge cells

Total RNA was extracted from pCas-*Bg*AIFx4-transfected and control Bge cells to assess the expression of Cas9, driven by the CMV promoter (Fig. 1B). Residual genomic DNAs were removed from the RNA samples by incubation with DNase I before reverse transcription was carried out. The resulting cDNAs from the control WT, mock-transfected and pCas-*Bg*AIFx4-transfected Bge cells were employed as the template in PCRs using two primer pairs, one specific for Cas9 and the other for *Bg*Actin, the actin gene of *B. glabrata* that served as the reference gene (Fig. 1B, C). Transcripts encoding Cas9 were detected at 24 hrs after transfection of the Bge cells, in each of 12 independent (biological) replicates (Figs. 1, 2). Subsequently, Cas9 transcripts were also detected on each of day from two to nine following transfection with pCas-*Bg*AIFx4, when the experiment was terminated (Fig. 1C; 231 bp amplicon, arrow). By contrast, Cas9-specific transcripts were not detected on any of the nine days in the control WT and the mock-treated groups of Bge cells. Expression of *Bg*Actin was seen in all three groups, the WT, mock-treated and pCas-*Bg*AIFx4-treated Bge cells, at each time point, confirming the integrity of the RNA samples (Fig. 1C; 214 bp amplicon, arrow).

Programmed mutation of *Bg*AIF confirmed functional CRISPR/Cas9 activity in *B. glabrata*

Genomic DNAs from control WT, mock-transfected and pCas-*Bg*AIFx4-transfected cells were employed as the template for PCRs employing the primer pair, AIF-F and AIR-R, which flank the programmed cleavage site in *Bg*AIF, exon 4 (Fig. 1A, green arrows; amplicon size, ~200 nt). The predicted site of the Cas9-catalyzed double strand break (DSB) in the *Bg*AIF locus is indicated in Fig. 1A with the red arrow. The nucleotide sequence of the amplicons was determined by Sanger direct sequencing using the same primers, AIF-F and AIF-R. The chromatograms of the sequence traces were inspected and analyzed for programmed CRISPR/Cas9-catalyzed mutations using the online ICE and TIDE tools (Brinkman & van Steensel, 2019; Brinkman *et al.*, 2018), which also include a decomposition algorithm to identify

the major, programmed mutations in the experimental when compared with the two control groups. The analysis identifies the editing site and quantifies the frequency of programmed mutations in a cell population. The online analyses revealed that transfection of Bge cells with the pCas9-*Bg*AIFx4 construct induced programmed mutations of the *Bg*AIF gene with an on-target CRISPR efficiency in each of the 12 biological replications, ranging from 8.9% to 17.1% INDELs (Fig. 2A, B) by TIDE and ICE analysis. Notably, the mutation profile in the vicinity of the predicted DSB in *Bg*AIF was similar in each of the biological replicates. Commonly seen INDELs at the DSBs site as revealed by the ICE analysis included deletions of 8 to 30 bp and insertions of 1 or 2 bp (Fig. 2A). The mutations were predicted to result in frame shift mutations, with consequent loss of the open reading frame and permanent loss of expression of *Bg*AIF in the mutant cell. The profile of frequency of mutations observed in each biological replicate was used to plot the curve (Prism v8 software) presented in Figure 2B. We concluded from these assays that programmed genome editing using CRISPR/Cas9 was active in *B. glabrata* Bge cells, and that the non-homologous end joining (NHEJ) pathway (Symington & Gautier, 2011) was active in *B. glabrata* to repair programmed double stranded breaks, leading to targeted gene knockout.

Programmed mutation interrupted expression of *Bg*AIF

Transcript levels encoding *Bg*AIF were assessed in the total RNAs of the Bge cells at nine days following transfection. Comparison of the experimental and control groups revealed significantly reduced levels of the *Bg*AIF transcript in the pCas-*Bg*AIFx4-transfected cells, mean 49.55±20.22%, range 28.1-86.3%, n =12 compared to the mock-treated control cells (unpaired *t*-test, t = 8.584, df = 22, $P \leq 0.05$) (Fig. 1B). There was no correlation apparent between the percentage INDELs and transcript reductions (not shown).

Programmed knockout of *Bg*AIF interfered with adherence of Bge cells to schistosome sporocysts

Single cell suspensions of Bge cells in the WT, mock-treated and Δ*Bg*AIF groups were co-cultured in siliconized tubes with primary *S. mansoni* sporocysts for 24 hrs. At that point, the numbers of cells that had adhered to each sporocyst were scored. This was accomplished by examination of at least five discrete sites of the well of the 24-well plate with more than 50 sporocyst of each group. The cell adhesion index (CAI) were scored from 1 to 4, with a score of 1 indicating few or no adherence cells and a score of 4 indicating that more than half the tegumental surface of the sporocyst was covered in cells or clumps of cells, as established in earlier reports (Fig. 3A). Cells from WT and mock-transfected controls mostly adhered in clumps or singly to the surface of the parasite (representative images in the upper panels of Fig. 3B), with CAI values that ranged from 2 to 4. By contrast, fewer cells adhered to the surface of the sporocysts in the Δ*Bg*AIF-Bge group (representative images, lower panels in Fig. 3B), with CAI values ranging from 2 to 3. Only ~20% of the Δ*Bg*AIF-Bge cells adhered to the surface of the parasite, and most of the cells retained single cell spread through the tissue culture well (Fig. 3B). More specifically, the mean CAI values ascertained from the seven biological replicates (≥50 parasites in each replicate (>400 parasites scored), mean 2.66±0.10, range, 2.53 to 2.78 in both the WT and mock-transfected control groups were significantly higher than the Δ*Bg*AIF

group, mean. 2.25±0.22, range, 2.08 to 2.55 (Fig 3C) ($P \leq 0.01$, unpaired *t*-test). Morphological changes among the Δ*Bg*AIF-Bge cells and the control group cells were not apparent.

Discussion

This report describes a novel use of programmed genome editing by the CRISPR/Cas9 approach in the gastropod snail, *B. glabrata*, an intermediate host snail of the human blood fluke, *S. mansoni*. The embryonic cell line from *B. glabrata*, termed the Bge line, is a valued tool for investigation of snail-schistosome, host-parasite interactions. A key attribute of the Bge cell is its hemocyte-like phenotype, given the central role of the snail hemocyte in innate and cellular immunity. The allograft inhibitory factor 1 (AIF, *aif*) is a conserved calcium-binding protein typically expressed in phagocytic and granular leukocytes and is a marker of macrophage activation (Zhang *et al.*, 2008; Zhang *et al.*, 2013; Chen *et al.*, 2012; Donovan *et al.*, 2018; De Zoysa *et al.*, 2010; Li *et al.*, 2016; Liu *et al.*, 2007; Schorn *et al.*, 2015). AIF is highly expressed in isolates of *B. glabrata* that are resistant to infection with *S. mansoni* (Lockyer *et al.*, 2012; Larson *et al.*, 2014). Here, we targeted the *aif* gene of *B. glabrata* for programmed gene knockout.

We constructed a plasmid vector encoding the CRISPR/Cas9 nuclease and a guide RNA targeting exon 4 of *Bg*AIF gene and *S. pyogenes* Cas9 nuclease, and transfected Bge cells with the gene-editing construct by square wave electroporation. Transcript levels of *Bg*AIF were significantly reduced by up to 73% following transformation. In parallel, sequence reads of amplicons spanning the locus targeted from programmed gene knock-out revealed on-target mutation on the *Bg*AIF gene, that had been repaired by non-homologous end joining leading to gene-inactivating insertions and deletions. In addition, the adherence of gene-edited Bge cells to sporocysts was significantly impeded in comparison to control cells, as ascertained using a semi-quantitative, cell adherence index .

These findings also confirmed the tractability of transfection of Bge cells by electroporation with the genome-editing construct, pCas-*Bg*AIFx4, and that the CMV promoter drove transcription of Cas9 in this snail species. Whereas transformation by plasmid DNA of Bge cells by square wave electroporation appears to be novel, Bge cells have been transformed in earlier reports using DNA complexed with cationic lipid-based transfection reagents and with polyethyleneimine (Rinaldi *et al.*, 2015). However, there are some limitations to our study. We were not be able to enrich the transfected cells from wild type cells. Future studies using a drug selectable marker may address this impediment (Rinaldi *et al.*, 2015). Also, other approaches for delivery of the CRISPR/Cas9 gene editing nuclease and guide might be tried, including repeated inoculation with ribonuclear protein complexes (Lin *et al.*, 2014) and or transduction by lentiviral virions encoding the gRNA and S. pyogenes Cas9 nuclease as we demonstrated with eggs *of S. mansoni* (Ittiprasert *et al.*, 2019).

To conclude, here we provide a demonstration of gene editing in a medically important taxon of freshwater gastropods that are necessary for the transmission of schistosomiasis. In like fashion, functional genomics using CRISPR/Cas9 genome editing that schistosomes and other trematodes responsible for major neglected tropical diseases have been reported (Arunsan *et al.*, 2019; Ittiprasert *et al.*, 2019). Accordingly, it may not be feasible to address fundamental questions in in this host-parasite relationship using genetically modified snails and schistosomes.

Acknowledgments

We thank Dr. Mathilde Knight for informative discussions on the snail-schistosome immunobiology and Dr. Margaret Mentink-Kane for support with the Bge cell line. Bge cells were provided by the NIAID Schistosomiasis Resource Center of the Biomedical Research Institute, Rockville, Maryland through NIH-NIAID contract HHSN272201000005I for distribution through BEI Resources. This work was supported by the Wellcome Trust Strategic Award no. 107475/Z/15/Z, Functional Genomics Flatworms Initiative (FUGI) (Hoffmann, K.H., principal investigator), the Coordenação de Aperfeiçoamento de Pessoal de Nível Superior (CAPES) - finance code 001 and Productivity fellowship from Conselho Nacional de Desenvolvimento Científico e Tecnológico (CNPq) granted to MMM (302518/2018-5), Brasil.

Figure legends

Figure 1. Schematic diagram of *Bg*AIF gene structure, CRISPR/Cas9 vector and expression in Bge cell. Panel **A**. Gene structure of *B. glabrata* allograft inflammatory factor (*Bg*AIF), accession number BGLB005061 and gene editing target locus (red box) on exon 4. *Bg*AIF gene composed of 5 exons and 4 introns. The green arrows indicate the location of primers flanking expected DSBs which were used in PCR to generate the on-target amplicon for INDELs estimation. **B.** Map of the pCas-*Bg*AIFx4 vector which includes the Pol III-dependent mammalian U6 gene promoter (red arrow) to drive transcription of the guide RNA targeting exon 4 of *Bg*AIF gene (red arrow) and the CMV promoter to drive expression of the *S. pyogenes* Cas9 nuclease (blue arrow). Primer pairs specific for the guide RNA and for Cas9 are indicated (green arrows). **C**. Expression of Cas9 and of *Bg*Actin (as the reference gene) transcripts as established by semi-quantitative RT-PCR in pCas-*Bg*AIF-transfected (right) and control (left) Bge cells from days one to nine following transfection. The Amplicons of the expected sizes, 231 bp for Cas9 and 214 pb for *Bg*Actin are as indicated. All RNA samples were positive for the *Bg*Actin reference at 214 bp band.

Figure 2. Establishment of *Bg*AIF-knockout lines of Bge cells. Panel **A**. Representative examples of frequent gene insertions-deletions (1-2 bp insertions and 8-30 bp deletions, straddling the programmed CRISPR/Cas9-induced double stranded break in exon 4, as determined by online ICE software-based analysis. **B.** TIDE algorithm-based violin plot of insertion-deletion percentages (%INDEL) computed using the amplicon sequence traces from the 12 biological replicates of pCas-*Bg*AIF-transfected Bge cell populations. **C.** Reduction of *Bg*AIF transcription by about 50% following programmed genome editing of Bge cells (Δ*Bg*AIF-Bge) in comparison to control Bge cells. Mean transcript reduction, 49.55± 20.22 (S.D.) percent, $P \leq 0.0001$ (****), n =12 (unpaired Student's *t*-test).

Figure 3. Programmed knockout of *Bg*AIF in Bge cells caused reduced adherence to primary sporocysts. Panel **A**. Representative micrographs of primary sporocysts co-cultured with Bge cells in our laboratory to profile the semi-quantitative scoring of the cell adhesion index (CAI); CAI value = 1; no cell adhering to the surface of the sporocyst; value = 2; ≤10 cells adhering to the sporocyst; value = 3; > 10 cells < half of the sporocyst surface covered by cells or clumps of cells; value = 4; > half the sporocyst surface covered by Bge cells (Castillo & Yoshino, 2002). **B**. Representative micrographs to indication the reduced levels of adherence of Δ*Bg*AIF-Bge cells (right panel) in comparison to control, mock-transfected Bge cells (left panel) to the co-cultured sporocysts. **C.** Bar chart to present the CAI values from control (mock-transfected) Δ*Bg*AIF-Bge cells during co-culture with primary sporocysts at a co-culture ratio of one sporocyst to 100 Bge cells; CAI value = 2.66±0.10, mean ±SD (476 sporocysts in total scored) for the mock-transfected Bge and 2.31±0.23 for the Δ*Bg*AIF-Bge cells (424 sporocysts in total scored); $P = 0.0033$, unpaired Student's *t* test; n =7 biological replicates.

References

[1] J.P. Webster, and C.M. Davies (2001). Coevolution and compatibility in the snail-schistosome system. *Parasitology* 123 Suppl, S41-56.

[2] A. El-Ansary, and S. Al-Daihan (2006). Important aspects of Biomphalaria snail-schistosome interactions as targets for antischistosome drug. *Med Sci Monit* 12, RA282-292.

[3] C.S. Richards, and P.C. Shade (1987). The genetic variation of compatibility in Biomphalaria glabrata and Schistosoma mansoni. *J Parasitol* 73, 1146-51.

[4] M. Knight, A. Miller, Y. Liu, P. Scaria, M. Woodle, and W. Ittiprasert (2011). Polyethyleneimine (PEI) mediated siRNA gene silencing in the Schistosoma mansoni snail host, Biomphalaria glabrata. *PLoS Negl Trop Dis* 5, e1212.

[5] L.K. Jannotti-Passos, H.M. Andrade, R.L. Caldeira, A.J. Romanha, S.M. Murta, D.A. Chapeaurouge, J. Perales, P.M. Coelho, and O.S. Carvalho (2008). Proteome analysis of the cardiac and pericardial tissue of Biomphalaria tenagophila populations susceptible and resistant to Schistosoma mansoni infection. *Acta Trop* 105, 229-34.

[6] P.C. Hanington, M.A. Forys, J.W. Dragoo, S.M. Zhang, C.M. Adema, and E.S. Loker (2010). Role for a somatically diversified lectin in resistance of an invertebrate to parasite infection. *Proc Natl Acad Sci U S A* 107, 21087-92.

[7] E.A. Pila, M.A. Gordy, V.K. Phillips, A.L. Kabore, S.P. Rudko, and P.C. Hanington (2016). Endogenous growth factor stimulation of hemocyte proliferation induces resistance to Schistosoma mansoni challenge in the snail host. *Proc Natl Acad Sci U S A* 113, 5305-10.

[8] S.M. Zhang, H. Nian, Y. Zeng, and R.J. Dejong (2008). Fibrinogen-bearing protein genes in the snail Biomphalaria glabrata: characterization of two novel genes and expression studies during ontogenesis and trematode infection. *Dev Comp Immunol* 32, 1119-30.

[9] A.E. Lockyer, A.M. Emery, R.A. Kane, A.J. Walker, C.D. Mayer, G. Mitta, C. Coustau, C.M. Adema, B. Hanelt, D. Rollinson, L.R. Noble, and C.S. Jones (2012). Early differential gene expression in haemocytes from resistant and susceptible Biomphalaria glabrata strains in response to Schistosoma mansoni. *PLoS One* 7, e51102.

[10] M.K. Larson, R.C. Bender, and C.J. Bayne (2014). Resistance of Biomphalaria glabrata 13-16-R1 snails to Schistosoma mansoni PR1 is a function of haemocyte abundance and constitutive levels of specific transcripts in haemocytes. *Int J Parasitol* 44, 343-53.

[11] S. Pinaud, J. Portela, D. Duval, F.C. Nowacki, M.A. Olive, J.F. Allienne, R. Galinier, N.M. Dheilly, S. Kieffer-Jaquinod, G. Mitta, A. Theron, and B. Gourbal (2016). A Shift from Cellular to Humoral Responses Contributes to Innate Immune Memory in the Vector Snail Biomphalaria glabrata. *PLoS Pathog* 12, e1005361.

[12] L. Barbosa, R.L. Caldeira, O.S. Carvalho, T.H. Vidigal, L.K. Jannotti-Passos, and P.M. Coelho (2006). Resistance to Schistosoma mansoni by transplantation of APO Biomphalaria tenagophila. *Parasite Immunol* 28, 209-12.

[13] C.M. Adema, and E.S. Loker (2015). Digenean-gastropod host associations inform on aspects of specific immunity in snails. *Dev Comp Immunol* 48, 275-83.

[14] C. Coustau, B. Gourbal, D. Duval, T.P. Yoshino, C.M. Adema, and G. Mitta (2015). Advances in gastropod immunity from the study of the interaction between the snail Biomphalaria glabrata and its parasites: A review of research progress over the last decade. *Fish Shellfish Immunol* 46, 5-16.

[15] G. Mitta, B. Gourbal, C. Grunau, M. Knight, J.M. Bridger, and A. Theron (2017). The Compatibility Between Biomphalaria glabrata Snails and Schistosoma mansoni: An Increasingly Complex Puzzle. *Adv Parasitol* 97, 111-145.

[16] E.A. Pila, H. Li, J.R. Hambrook, X. Wu, and P.C. Hanington (2017). Schistosomiasis from a Snail's Perspective: Advances in Snail Immunity. *Trends Parasitol* 33, 845-857.

[17] M. Knight, H.D. Arican-Goktas, W. Ittiprasert, E.C. Odoemelam, A.N. Miller, and J.M. Bridger (2014). Schistosomes and snails: a molecular encounter. *Front Genet* 5, 230.

[18] D.O. Famakinde (2017). Molecular context of Schistosoma mansoni transmission in the molluscan environments: A mini-review. *Acta Trop* 176, 98-104.

[19] R.E. Yescott, and E. Hansen (1976). Effect of manganese on Biomphalaria glabrata infected with Schistosoma mansoni. *Journal of invertebrate pathology* 28, 315-20.

[20] J.R. Laursen, and T.P. Yoshino (1999). Biomphalaria glabrata embryonic (Bge) cell line supports in vitro miracidial transformation and early larval development of the deer liver fluke, Fascioloides magna. *Parasitology* 118 (Pt 2), 187-94.

[21] N.J. Wheeler, N. Dinguirard, J. Marquez, A. Gonzalez, M. Zamanian, T.P. Yoshino, and M.G. Castillo (2018a). Correction to: Sequence and structural variation in the genome of the Biomphalaria glabrata embryonic (Bge) cell line. *Parasit Vectors* 11, 566.

[22] N.J. Wheeler, N. Dinguirard, J. Marquez, A. Gonzalez, M. Zamanian, T.P. Yoshino, and M.G. Castillo (2018b). Sequence and structural variation in the genome of the Biomphalaria glabrata embryonic (Bge) cell line. *Parasit Vectors* 11, 496.

[23] G. Rinaldi, H. Yan, R. Nacif-Pimenta, P. Matchimakul, J. Bridger, V.H. Mann, M.J. Smout, P.J. Brindley, and M. Knight (2015). Cytometric analysis, genetic manipulation and antibiotic selection of the snail embryonic cell line Bge from Biomphalaria glabrata, the intermediate host of Schistosoma mansoni. *Int J Parasitol* 45, 527-35.

[24] E. Odoemelam, N. Raghavan, A. Miller, J.M. Bridger, and M. Knight (2009). Revised karyotyping and gene mapping of the Biomphalaria glabrata embryonic (Bge) cell line. *Int J Parasitol* 39, 675-81.

[25] J.J. Vermeire, J.P. Boyle, and T.P. Yoshino (2004). Differential gene expression and the effects of Biomphalaria glabrata embryonic (Bge) cell factors during larval Schistosoma mansoni development. *Mol Biochem Parasitol* 135, 153-7.

[26] M.G. Castillo, and T.P. Yoshino (2002). Carbohydrate inhibition of Biomphalaria glabrata embryonic (Bge) cell adhesion to primary sporocysts of Schistosoma mansoni. *Parasitology* 125, 513-25.

[27] J.E. Humphries, L. Elizondo, and T.P. Yoshino (2001). Protein kinase C regulation of cell spreading in the molluscan Biomphalaria glabrata embryonic (Bge) cell line. *Biochim Biophys Acta* 1540, 243-52.

[28] T.P. Yoshino, and J.R. Laursen (1995). Production of Schistosoma mansoni daughter sporocysts from mother sporocysts maintained in synxenic culture with Biomphalaria glabrata embryonic (Bge) cells. *J Parasitol* 81, 714-22.

[29] C.M. Adema, L.W. Hillier, C.S. Jones, E.S. Loker, M. Knight, P. Minx, G. Oliveira, N. Raghavan, A. Shedlock, L.R. do Amaral, H.D. Arican-Goktas, J.G. Assis, E.H. Baba, O.L. Baron, C.J. Bayne, U. Bickham-Wright, K.K. Biggar, M. Blouin, B.C. Bonning, C. Botka, J.M. Bridger, K.M. Buckley, S.K. Buddenborg, R. Lima Caldeira, J. Carleton, O.S. Carvalho, M.G. Castillo, I.W. Chalmers, M. Christensens, S. Clifton, C. Cosseau, C. Coustau, R.M. Cripps, Y. Cuesta-Astroz, S.F. Cummins, L. di Stephano, N. Dinguirard, D. Duval, S. Emrich, C. Feschotte, R. Feyereisen, P. FitzGerald, C. Fronick, L. Fulton, R. Galinier, S.G. Gava, M. Geusz, K.K. Geyer, G.I. Giraldo-Calderon, M. de Souza Gomes, M.A. Gordy, B. Gourbal, C. Grunau, P.C. Hanington, K.F. Hoffmann, D. Hughes, J. Humphries, D.J. Jackson, L.K. Jannotti-Passos, W. de Jesus Jeremias, S. Jobling, B.

Kamel, A. Kapusta, S. Kaur, J.M. Koene, A.B. Kohn, D. Lawson, S.P. Lawton, D. Liang, Y. Limpanont, S. Liu, A.E. Lockyer, T.L. Lovato, F. Ludolf, V. Magrini, D.P. McManus, M. Medina, M. Misra, G. Mitta, G.M. Mkoji, M.J. Montague, C. Montelongo, L.L. Moroz, M.C. Munoz-Torres, U. Niazi, L.R. Noble, F.S. Oliveira, F.S. Pais, A.T. Papenfuss, R. Peace, J.J. Pena, E.A. Pila, T. Quelais, B.J. Raney, J.P. Rast, D. Rollinson, I.C. Rosse, B. Rotgans, E.J. Routledge, K.M. Ryan, et al. (2017). Whole genome analysis of a schistosomiasis-transmitting freshwater snail. *Nat Commun* 8, 15451.

[30] Y. Zhang, J. Li, F. Yu, X. He, and Z. Yu (2013). Allograft inflammatory factor-1 stimulates hemocyte immune activation by enhancing phagocytosis and expression of inflammatory cytokines in Crassostrea gigas. *Fish Shellfish Immunol* 34, 1071-7.

[31] Q.R. Chen, F. Guan, S.M. Song, J.K. Jin, D.S. Lei, C.M. Chen, J.H. Lei, Z.W. Chen, and A.O. Niu (2014). Allograft inflammatory factor-1 alleviates liver disease of BALB/c mice infected with Schistosoma japonicum. *Parasitol Res* 113, 2629-39.

[32] Q.R. Chen, F. Guan, D.J. Yan, D.S. Lei, L. Fu, H.S. Xia, Y.H. Zhu, Z.W. Chen, and A.O. Niu (2012). The dynamic expression of allograft inflammatory factor-1 in hepatic tissues and splenic cells of BALB/c mice with Schistosoma japonicum infection. *Tissue Antigens* 79, 33-41.

[33] J.A. Doudna, and E. Charpentier (2014). Genome editing. The new frontier of genome engineering with CRISPR-Cas9. *Science* 346, 1258096.

[34] F. Jiang, and J.A. Doudna (2017). CRISPR-Cas9 Structures and Mechanisms. *Annual review of biophysics* 46, 505-529.

[35] L. Cong, F.A. Ran, D. Cox, S. Lin, R. Barretto, N. Habib, P.D. Hsu, X. Wu, W. Jiang, L.A. Marraffini, and F. Zhang (2013). Multiplex genome engineering using CRISPR/Cas systems. *Science* 339, 819-23.

[36] K. Labun, T.G. Montague, M. Krause, Y.N. Torres Cleuren, H. Tjeldnes, and E. Valen (2019). CHOPCHOP v3: expanding the CRISPR web toolbox beyond genome editing. *Nucleic Acids Res* 47, W171-W174.

[37] K. Labun, T.G. Montague, J.A. Gagnon, S.B. Thyme, and E. Valen (2016). CHOPCHOP v2: a web tool for the next generation of CRISPR genome engineering. *Nucleic Acids Res* 44, W272-6.

[38] T.G. Montague, J.M. Cruz, J.A. Gagnon, G.M. Church, and E. Valen (2014). CHOPCHOP: a CRISPR/Cas9 and TALEN web tool for genome editing. *Nucleic Acids Res* 42, W401-7.

[39] P. Arunsan, W. Ittiprasert, M.J. Smout, C.J. Cochran, V.H. Mann, S. Chaiyadet, S.E. Karinshak, B. Sripa, N.D. Young, J. Sotillo, A. Loukas, P.J. Brindley, and T. Laha (2019). Programmed knockout mutation of liver fluke granulin attenuates virulence of infection-induced hepatobiliary morbidity. *Elife* 8.

[40] W. Ittiprasert, V.H. Mann, S.E. Karinshak, A. Coghlan, G. Rinaldi, G. Sankaranarayanan, A. Chaidee, T. Tanno, C. Kumkhaek, P. Prangtaworn, M.M. Mentink-Kane, C.J. Cochran, P. Driguez, N. Holroyd, A. Tracey, R. Rodpai, B. Everts, C.H. Hokke, K.F. Hoffmann, M. Berriman, and P.J. Brindley (2019). Programmed genome editing of the omega-1 ribonuclease of the blood fluke, Schistosoma mansoni. *Elife* 8.

[41] E.K. Brinkman, and B. van Steensel (2019). Rapid Quantitative Evaluation of CRISPR Genome Editing by TIDE and TIDER. *Methods Mol Biol* 1961, 29-44.

[42] E.K. Brinkman, A.N. Kousholt, T. Harmsen, C. Leemans, T. Chen, J. Jonkers, and B. van Steensel (2018). Easy quantification of template-directed CRISPR/Cas9 editing. *Nucleic Acids Res* 46, e58.

[43] T. Hsiau, T. Maures, K. Waite, J. Yang, R. Kelso, K. Holden, and R. Stoner (2018). Inference of CRISPR edits from Sanger Trace Data. *bioRxiv 251082; doi: https://doi.org/10.1101/251082*.

[44] K.J. Livak, and T.D. Schmittgen (2001). Analysis of relative gene expression data using real-time quantitative PCR and the 2(-Delta Delta C(T)) Method. *Methods* 25, 402-8.

[45] C.J. Bayne, E.S. Loker, M.A. Yui, and J.A. Stephens (1984). Immune-recognition of Schistosoma mansoni primary sporocysts may require specific receptors on Biomphalaria glabrata hemocytes. *Parasite Immunol* 6, 519-28.

[46] L.S. Symington, and J. Gautier (2011). Double-strand break end resection and repair pathway choice. *Annual review of genetics* 45, 247-71.

[47] K.M. Donovan, M.R. Leidinger, L.P. McQuillen, J.A. Goeken, C.M. Hogan, S.C. Harwani, H.A. Flaherty, and D.K. Meyerholz (2018). Allograft Inflammatory Factor 1 as an Immunohistochemical Marker for Macrophages in Multiple Tissues and Laboratory Animal Species. *Comparative medicine* 68, 341-348.

[48] M. De Zoysa, C. Nikapitiya, Y. Kim, C. Oh, D.H. Kang, I. Whang, S.J. Kim, J.S. Lee, C.Y. Choi, and J. Lee (2010). Allograft inflammatory factor-1 in disk abalone (Haliotis discus discus): molecular cloning, transcriptional regulation against immune challenge and tissue injury. *Fish Shellfish Immunol* 29, 319-26.

[49] Q. Li, Z. Bai, L. Zhao, and J. Li (2016). Characterization of allograft inflammatory factor-1 in Hyriopsis cumingii and its expression in response to immune challenge and pearl sac formation. *Fish Shellfish Immunol* 59, 241-249.

[50] G. Liu, H. Ma, L. Jiang, and Y. Zhao (2007). Allograft inflammatory factor-1 and its immune regulation. *Autoimmunity* 40, 95-102.

[51] T. Schorn, F. Drago, G. Tettamanti, R. Valvassori, M. de Eguileor, J. Vizioli, and A. Grimaldi (2015). Homolog of allograft inflammatory factor-1 induces macrophage migration during innate immune response in leech. *Cell and tissue research* 359, 853-64.

[52] S. Lin, B.T. Staahl, R.K. Alla, and J.A. Doudna (2014). Enhanced homology-directed human genome engineering by controlled timing of CRISPR/Cas9 delivery. *Elife* 3, e04766.

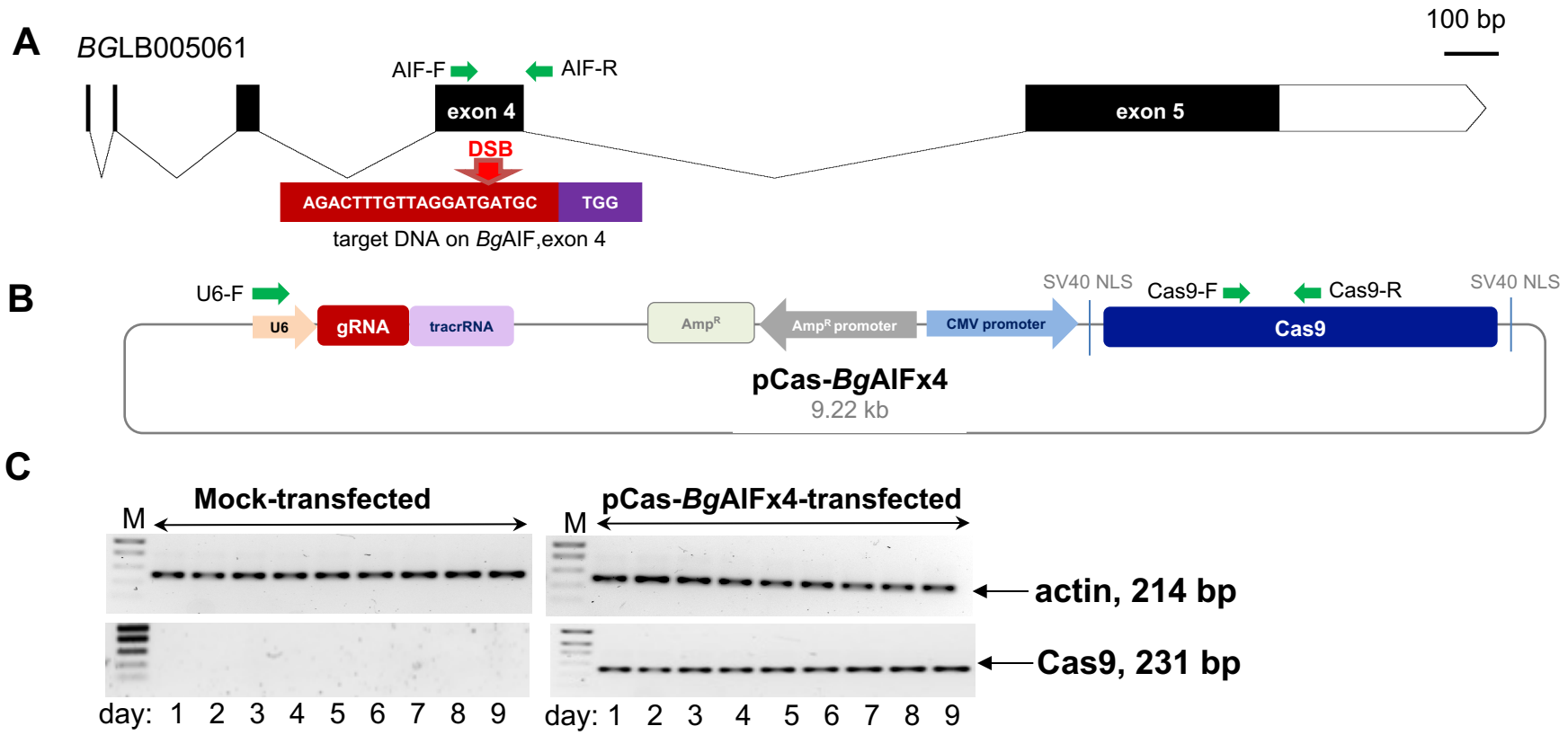
A
BGLB005061
100 bp
AIF-F
AIF-R
exon 4
exon 5
DSB
AGACTTTGTTAGGATGATGC
TGG
target DNA on BgAIF,exon 4
B
U6-F
U6
gRNA
tracrRNA
AmpR
AmpR promoter
CMV promoter
SV40 NLS
Cas9-F
Cas9-R
SV40 NLS
Cas9
pCas-BgAIFx4
9.22 kb
C
Mock-transfected
pCas-BgAIFx4-transfected
M
M
actin, 214 bp
Cas9, 231 bp
day: 1 2 3 4 5 6 7 8 9
day: 1 2 3 4 5 6 7 8 9

Figure 1

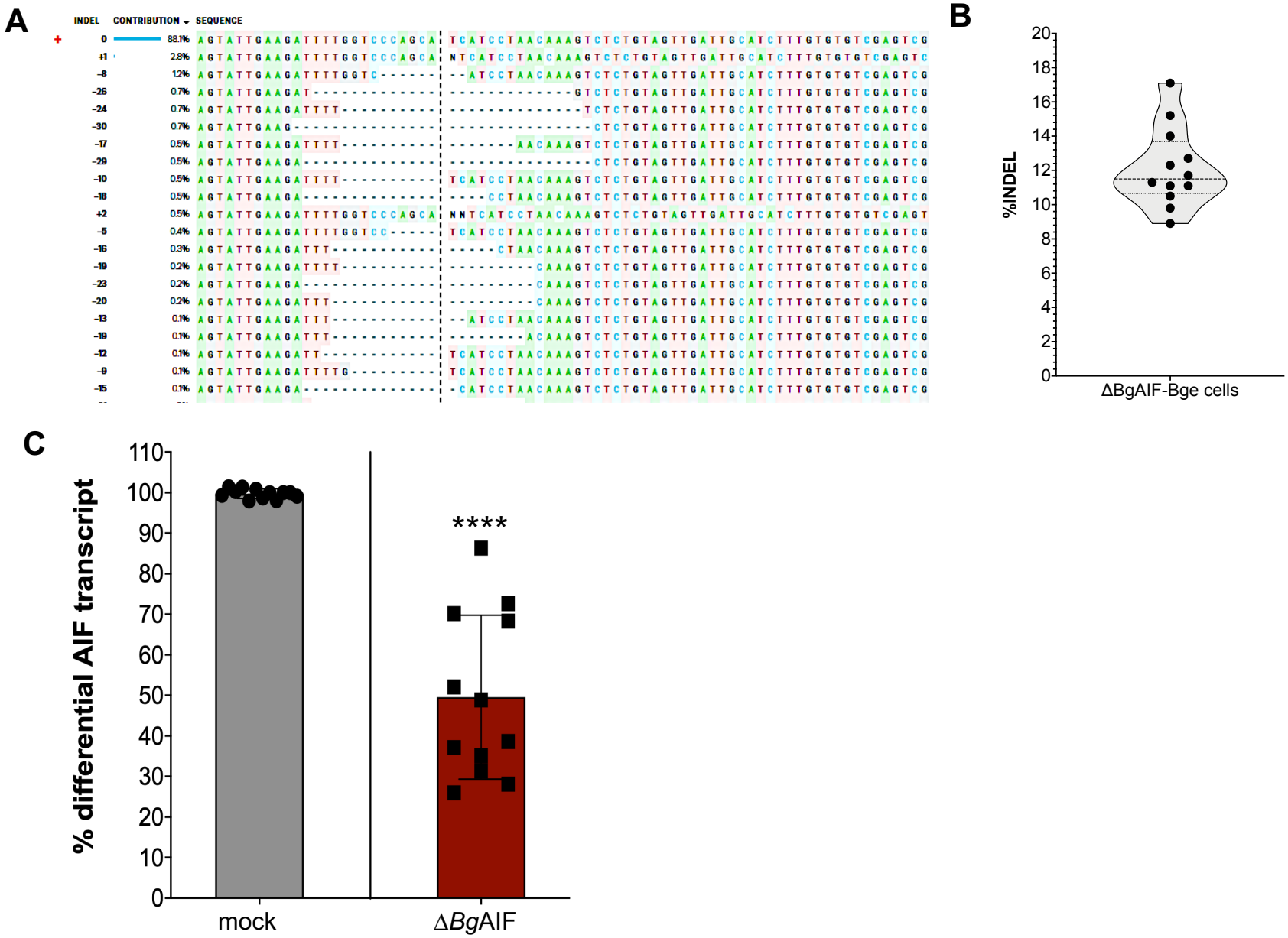
A
INDEL
CONTRIBUTION
SEQUENCE
B
%INDEL
ΔBgAIF-Bge cells
C
% differential AIF transcript
****
mock
ΔBgAIF

Figure 2

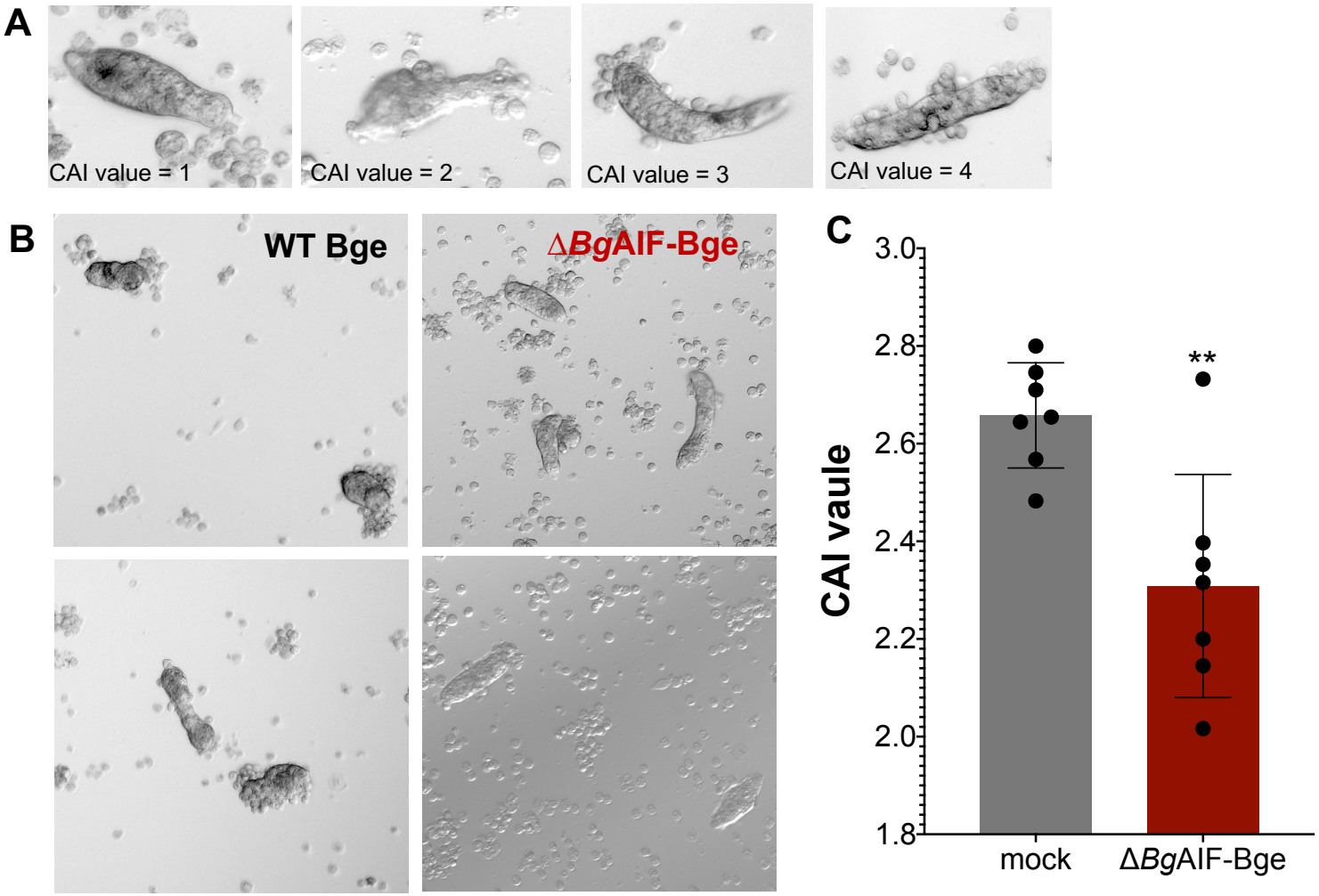
A
CAI value = 1
CAI value = 2
CAI value = 3
CAI value = 4
B
WT Bge
ΔBgAlF-Bge
C
CAI vaule
3.0
2.8
2.6
2.4
2.2
2.0
1.8
**
mock
ΔBgAlF-Bge

Figure 3